

Structural colour printing using a magnetically tunable and lithographically fixable photonic crystal

Hyoki Kim¹, Jianping Ge², Junhoi Kim¹, Sung-eun Choi¹, Hosuk Lee¹, Howon Lee¹, Wook Park¹, Yadong Yin² and Sunghoon Kwon^{1*}

Many creatures in nature, such as butterflies and peacocks, display unique brilliant colours, known as ‘structural colours’, which result from the interaction of light with periodic nanostructures on their surfaces. Mimicking such nanostructures found in nature, however, requires state-of-the-art nanofabrication techniques that are slow, expensive and not scalable. Herein, we demonstrate high-resolution patterning of multiple structural colours within seconds, based on successive tuning and fixing of colour using a single material along with a maskless lithography system. We have invented a material called ‘M-Ink’, the colour of which is tunable by magnetically changing the periodicity of the nanostructure and fixable by photochemically immobilizing those structures in a polymer network. We also demonstrate a flexible photonic crystal for the realization of structural colour printing. The simple, controllable and scalable structural colour printing scheme presented may have a significant impact on colour production for general consumer goods.

Structural colours in nature, such as those on butterfly wings, beetle cuticles and peacock feathers, have attracted considerable attention in a variety of research areas^{1–6}. Structural colour has many characteristics that differ from those of chemical pigments or dyes. For example, in the feathers of a peacock, various colours result from the interaction of light with a single biological material: melanin rods. The iridescent colours are formed as a result of the lattice spacing of the rods⁵. In nature, a single biological material with different physical configurations displays various colours, which greatly simplifies the manufacturing process in producing multiple colours. The unique colours originating from the physical structures are iridescent and metallic, and cannot be mimicked by chemical dyes or pigments. Furthermore, structural colour is free from photobleaching, unlike traditional pigments or dyes.

Owing to its unique characteristics, there have been many attempts to make artificial structural colour through various technological approaches such as colloidal crystallization^{7–20}, dielectric layer stacking^{21,22} and direct lithographic patterning^{23,24}. The colloidal crystallization technique is most frequently used to make a photonic crystal, which blocks a specific wavelength of light in the crystal and therefore displays the corresponding colour. Gravitational force⁷, centrifugal force⁸, hydrodynamic flow⁹, electrophoretic deposition¹⁰ and capillary force from the evaporation of solvents^{11–20} are used to assemble the colloidal crystals. Although these methods produce structural colours with a large area, the growth of colloidal crystals usually takes a long time so as to achieve better crystallization and fewer defects. Also, because the bandgap of a photonic crystal is dependent on the size of the colloids used, different sizes of colloidal suspensions are needed to produce multicoloured structures. Furthermore, there have been great technological difficulties in assembling colloids of different sizes to form these multicoloured patterns with fine resolutions.

Dielectric layer stacking and lithographic patterning of periodic dielectric materials generates structural colour by directly

controlling the submicrometre structure of the surface. Various fabrication processes have been reported, including replicating natural substrates²¹, depositing materials layer by layer²² and etching a substrate using various lithographic techniques^{23,24}. These approaches are advantageous in that they accurately fabricate a periodic dielectric structure on the surface, which controls the desired photonic bandgap. However, in spite of the advantage of sculpting sophisticated nanostructures in a well controlled manner, a cost-effective manufacturing scheme to generate multi-coloured structures over a large area is hard to achieve owing to the requirement for a vacuum process. Moreover, great effort and long process times are necessary to produce multicoloured patterns on a substrate, because different pitches of dielectric stacks are required to achieve different colours. Here, we present new material systems and instrumentation to overcome limitations to previous approaches, and demonstrate rapid production of high-resolution patterns of multiple structural colours. Photonic crystals with different bandgaps are formed on various substrates using a single magnetically active material and maskless lithography, within a few seconds.

The material developed in this work is a photonic crystal, termed M-Ink, the colour of which is magnetically tunable and lithographically fixable. M-Ink is a three-phase material system consisting of superparamagnetic colloidal nanocrystal clusters (CNCs), solvation liquid and photocurable resin (Fig. 1b). The superparamagnetic CNCs, each consisting of many single-domain magnetite nanocrystals, are capped with silica shells^{25,26}. Without an applied external magnetic field, the CNCs are randomly dispersed in liquid resin and display a brown colour, which is the intrinsic colour of magnetite. Under an external magnetic field, the CNCs are assembled to form chain-like structures along the magnetic field lines^{27,28}. An attractive magnetic force due to the superparamagnetic core is balanced with repulsive electrostatic and solvation forces. The combination of attractive and repulsive forces determines the interparticle distance, and the interparticle distance in a chain

¹School of Electrical Engineering and Computer Science, Seoul National University San 56-1, Shillim 9-dong, Gwanak-ku, Seoul 151-744, South Korea,

²Department of Chemistry, University of California Riverside, California 92521, USA. *e-mail: skwon@snu.ac.kr

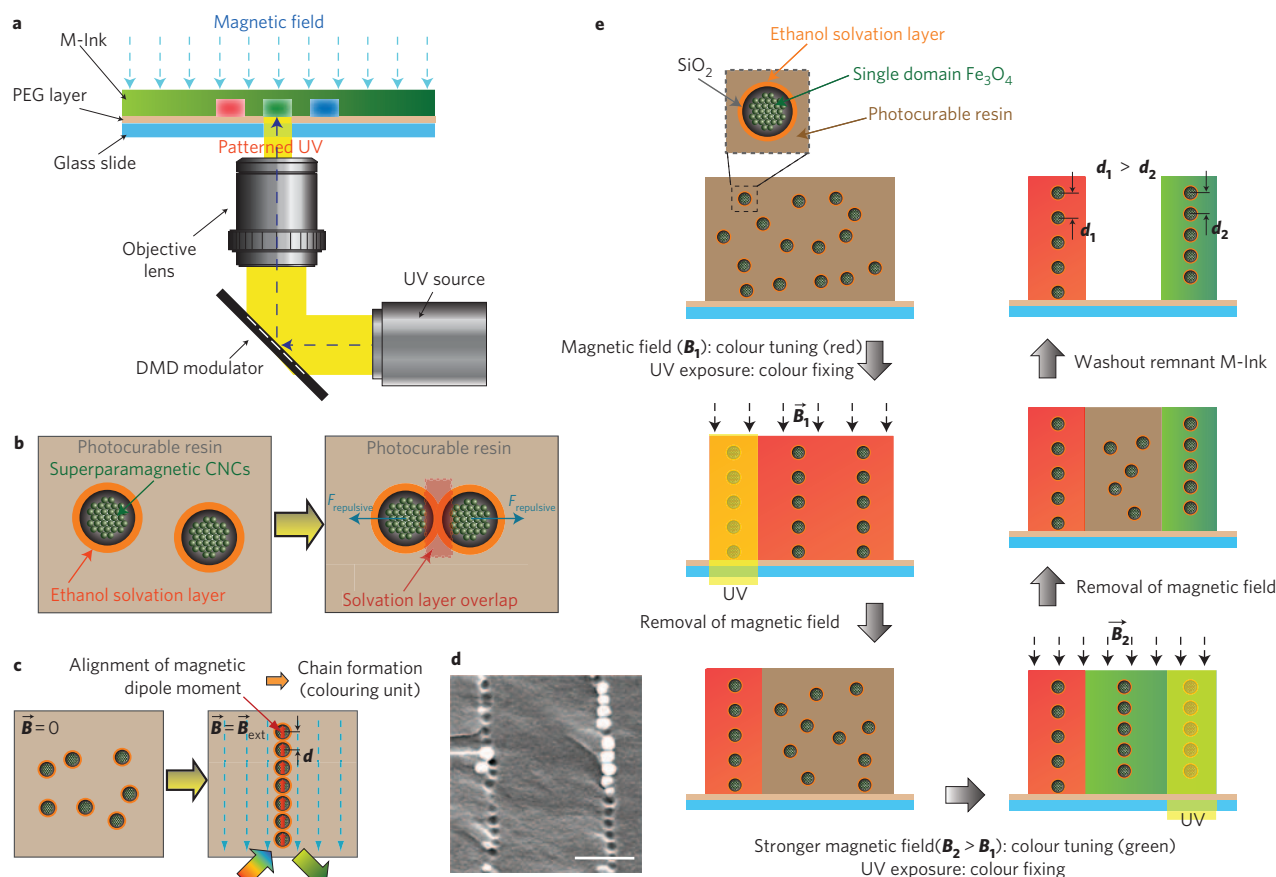


Figure 1 | Schematic of the production of high-resolution multiple structural colours with a single material. **a**, Maskless lithography setup for colour fixing. Instantaneous exposure using patterned UV light reflected from a digital micromirror array (DMD) modulator allows the fast production of structural colour. **b**, The superparamagnetic core and ethanol solvation layer allow the stable dispersion of the CNCs in the M-Ink. A strong repulsive force can be generated when two solvation layers overlap. **c**, Upon the application of an external magnetic field, CNCs are assembled to form a chain-like photonic nanostructure. This chain-like photonic nanostructure acts as a colouration unit of M-Ink, the colour of which can be tuned by varying the interparticle distance by modulation of the external magnetic field intensity. **d**, SEM image of a cross-section of the colour fixed structure. The dimpled structures are the traces of the chain-like aligned CNCs (scale bar 1 μm). **e**, Multicolour patterning of structural colour with a single material by the sequential steps of 'tuning and fixing'. The diffraction wavelength is tuned by varying the strength of the magnetic fields. Different interparticle distances determine the diffracted wavelength of the light, with shorter diffracted wavelength corresponding to shorter interparticle distance. Spatially patterned UV light polymerizes the M-Ink and fixes the position of ordered CNCs.

determines the colour of the light diffracted from the chain, which can be explained by Bragg diffraction theory (Fig. 1c). Thus, the colour can be tuned by simply varying the interparticle distance using external magnetic fields. Note that the solvation liquid is crucial for this material system, because a simple two-phase mixture, or dispersion of CNCs in photocurable resin without solvation liquid, does not possess strong and long-range repulsive interparticle forces that can cooperate with the magnetically induced attractive force to allow dynamic tuning. Without a strong repulsion force, the CNCs irreversibly aggregate with one another when they are pushed together upon application of the external magnetic fields^{29,30}. As illustrated in Fig. 1b, strong hydrogen-bonding solvents such as alkanols can form a relatively thick solvation layer around the CNCs' surface, which can provide strong repulsion when two solvation layers overlap²⁶. This three-phase system—the M-Ink composed of CNCs, ethanol and the photocurable resin—can successfully stabilize the CNCs and maintain colour tunability (see Supplementary Fig. S1, Section S1).

Once the desired colour is obtained from M-Ink by application of an external magnetic field, it can be fixed by solidifying the photocurable resin through ultraviolet (UV) exposure. The chain-like self-assembled CNCs can be frozen in the solidified polymer network

without distorting its periodic arrangements, thus retaining the structural colour. In comparison to the other solidification methods such as thermal curing, photocuring is instantaneous and can 'freeze' the self-assembled photonic nanostructure fast enough to prevent distortion³¹. Because of its instantaneous nature, photocuring also allows localized solidification for high-resolution patterning by avoiding significant free-radical diffusion during polymerization³². We use a maskless lithography system to focus UV energy to fix the colour from self-assembled chain-like photonic nanostructures (Fig. 1a). A fast microelectromechanical system (MEMS)-based spatial light modulator inside the system provides instantaneous illumination (<80 ms) of patterned UV light to the photocurable resin^{33,34}. Using this system, the chain-like structure can be preserved without distortion (Fig. 1d). Compared with traditional methods for generating structural colour by the slow growth of colloidal photonic crystals, magnetic assembly followed by photochemical immobilization was accomplished within seconds, with a high degree of spatial control (see Supplementary Fig. S3, Section S1).

The key idea of this work is the generation of multicoloured high-resolution patterns using M-Ink by repetitive tuning and fixing of the structural colour. Various multicoloured patterns can be generated

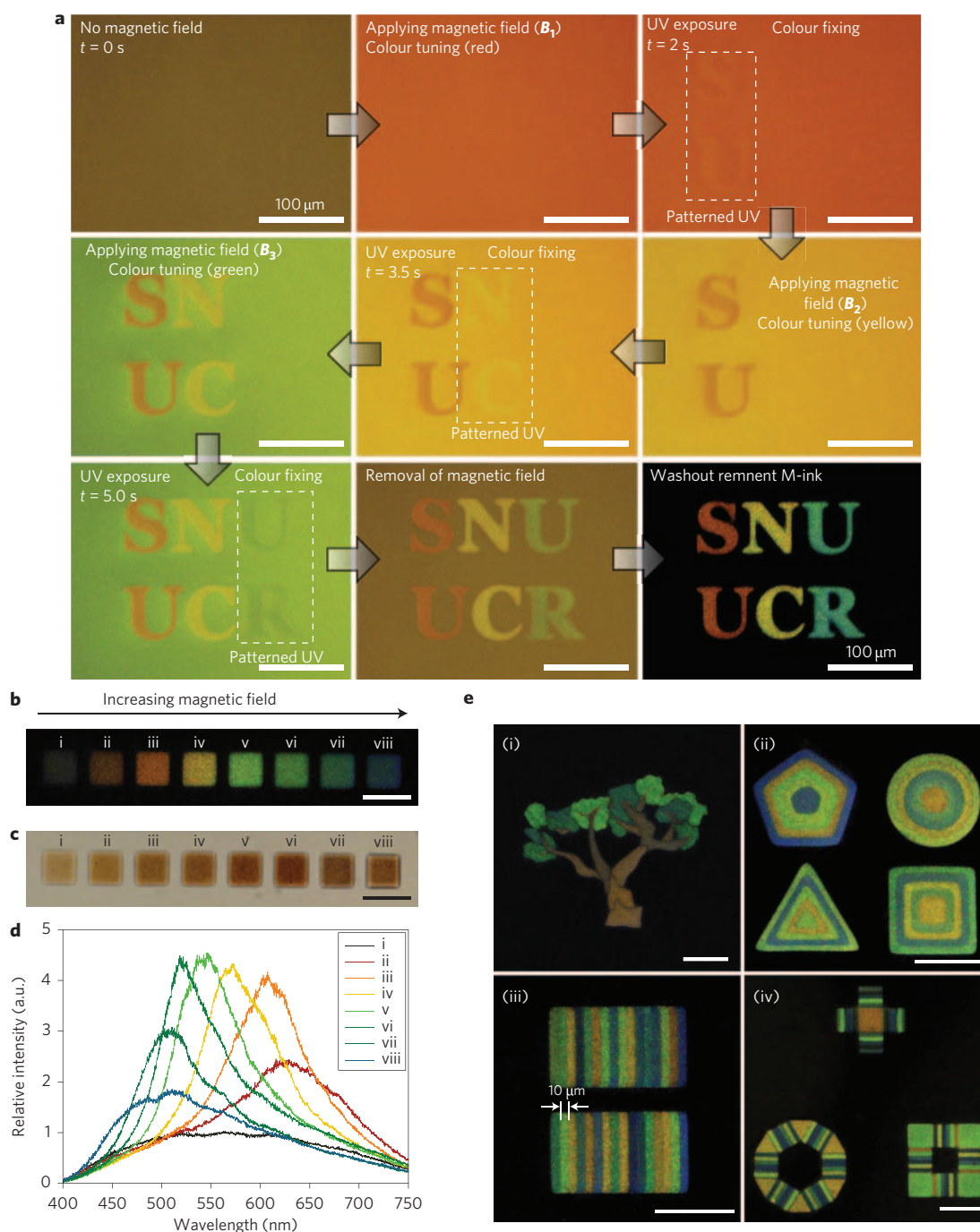


Figure 2 | Generation of high-resolution multiple structural colour patterns using M-Ink. **a**, Rapid production of high-resolution multiple structural colour.

A series of optical microscope images shows that the patterning of multiple structural colour with arbitrary features is completed within seconds.

b, Reflection micrographs of multicoloured structural colour generated by gradually increasing magnetic fields. Microstructure i is generated under the influence of no magnetic field. Microstructures ii–viii are generated under gradually increasing magnetic field strengths from 130 G to 700 G (scale bar 100 μm).

c, Transmission micrograph of the same sample as **a** (scale bar 100 μm). **d**, Corresponding spectra of the microstructures. Microstructure i does not show any diffraction peak in the visible range. Microstructures ii–viii show the shift of the diffraction peak to the shorter wavelength.

e, A tree (i), concentric patterns of triangles, squares, pentagons and circles (ii), multicoloured bar codes (iii), and composite patterns of strip and polygon (iv) (ii, iii, scale bars 100 μm ; i, iv, scale bars 250 μm).

with a single material by means of a sequential process involving cooperative actions of magnetic field modulation and spatially controlled UV exposure (Fig. 1e). We used a poly(ethylene glycol) (PEG)-coated glass slide as a substrate to avoid adhesion of the CNCs onto the surface of the bare glass slide (see Supplementary Fig. S2, Section S1). A thin layer of M-Ink was then deposited on the substrate. Once a desired colour of M-Ink was obtained by

exerting a magnetic field, the patterned UV exposure fixed the colour locally, producing a coloured pattern at specific regions. The colour of uncured M-Ink could then be changed simply by varying the strength of the magnetic field. Subsequent focused UV exposure produced another coloured pattern in a different location. As illustrated by Fig. 1e, micropatterns with different structural colours can be easily formed by repeating this ‘tuning and fixing’ process.

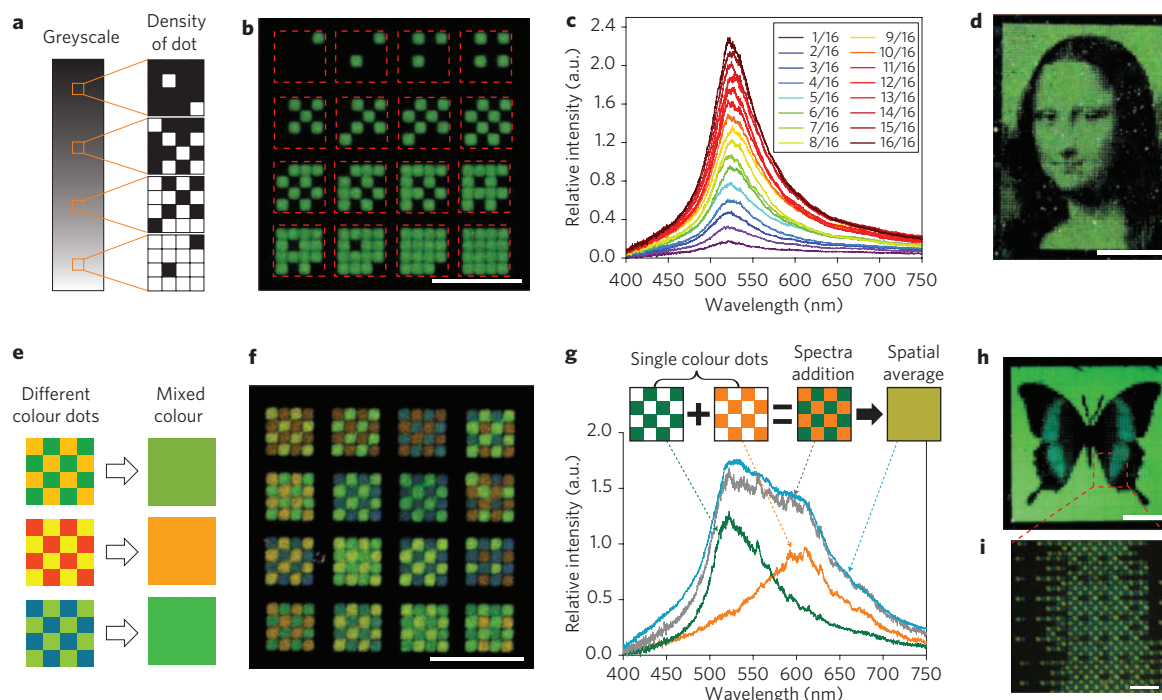


Figure 3 | Reflection intensity modulation and spatial colour mixing of structural colour. **a**, Schematic showing the expression of greyscale by varying dot density. **b**, Four-bit reflection intensity modulation by varying the number of monotone structural colour dots. Each of the red dotted lines indicates a pixel, showing distinct levels of reflection intensity (scale bar 250 μm). **c**, Reflectance spectra of the corresponding 16 pixels of **a**. **d**, Monotone 4-bit image of Mona Lisa, consisting of 4,800 pixels (scale bar 2 mm). **e**, Schematic showing the expression of colour mixing by the spatial distribution of different colour dots, the size of which should be smaller than the resolution of the human eye. **f**, Spatial colour mixing of structural colour. Each pixel of a 4×4 matrix consists of different colour dots, each of which is $\sim 25 \mu\text{m}$ in size (scale bar 250 μm). **g**, Corresponding reflectance spectra of selected pixels. Different colour dots make a single mixed spectrum. **h**, Reproduction of the butterfly *Papilio palinurus*. The colour of the wings in the reproduced image demonstrates structural colour mixing by mixing blue and yellow-green (scale bar 1 mm). **i**, A magnification of the indicated wing area of **h** consists of blue and yellow-green dots. Each dot has dimensions of $16.7 \times 16.7 \mu\text{m}^2$ ($\sim 1,500$ dpi) (scale bar 100 μm).

No movement of the substrate is required for deposition of multiple ink materials, because M-Ink is deposited only once at the beginning of the process. Also, multiple patterns can be exposed without moving either the substrate or the mask, because the maskless lithography system dynamically controls the pattern of multiple UV exposures without the need to physically change the photomasks. Therefore, our method combines the advantages of the M-Ink and a maskless lithography system, and can achieve high-resolution heterogeneous patterning rapidly, by eliminating the need for additional alignment and registration.

To demonstrate the concept of rapid patterning of multiple structural colours with a single ink, a multicolour pattern 'SNU/UCR' was produced using the sequential colour tuning and fixing process, which is shown in Fig. 2a as a series of fabrication steps. Note that the production of these multiple photonic crystal structures requires only a few seconds, clearly outpacing any other existing fabrication technologies for photonic crystals (see Supplementary Movie S1).

Figure 2b presents a reflective optical microscope image and Fig. 2d the corresponding spectrum data for each microstructure, showing gradual colour changes from red to blue as the applied magnetic field strength is gradually increased. This gradual increase in the external magnetic field induces an increasing attractive force between the induced magnetic dipole moment of the CNCs, thereby decreasing the interparticle distance in the chains. In agreement with Bragg diffraction theory, the spectra blueshift as a result of the gradual decrease in the interparticle distance. Meanwhile, applying UV light to the chain-like aligned CNCs structure in a resin matrix, a slight spectral shift to shorter wavelengths was observed with increasing UV dose. Polymer shrinkage was observed from the spectral variation (see Supplementary Information, Section S2).

It is worth noting that this tuning of the colours of M-Ink does not suffer from hysteresis and is very reproducible owing to the superparamagnetic nature of CNCs. Furthermore, the wide tuning range, covering the whole visible spectrum, is a result of the strong magnetic attractive force arising from the superparamagnetic properties of M-Ink and the repulsive forces having comparable strength. In this case, the repulsion is composed of the relatively weak but long-range electrostatic force and the relatively strong but short-range solvation force resulting from the ethanol solvation layer of the M-Ink.

The colours of the corresponding microstructures shown by the transmission microscope (Fig. 2c) are all brownish, the intrinsic colour of magnetite, and are quite different from those of the reflective optical microscope image. This unique difference between the reflection image and the transmission image further proves the formation of structural colour, in which the colouration mechanism is not based on the absorption of light as in typical pigments and dyes (see Supplementary Information, Section S3). Because the photonic crystal structure can be frozen within the polymeric matrix, we are able to confirm the chain structures directly, which usually disassemble in solution after removal of the magnetic field. As shown in Fig. 1d, a scanning electron microscope (SEM) image of the sliced cross-section with microtome of the cured M-Ink reveals that the diffraction of structural colour does come from the periodic arrangement of the CNCs in the chain. The dimpled structures of the sliced cross-sectional plane are the traces of the ordered CNCs. Also, this shows that the photopolymerization by the maskless lithography system preserves the original chain structure formed in the liquid phase.

By controlling the UV exposure pattern and magnetic field strength, we produced high-resolution patterns of multiple

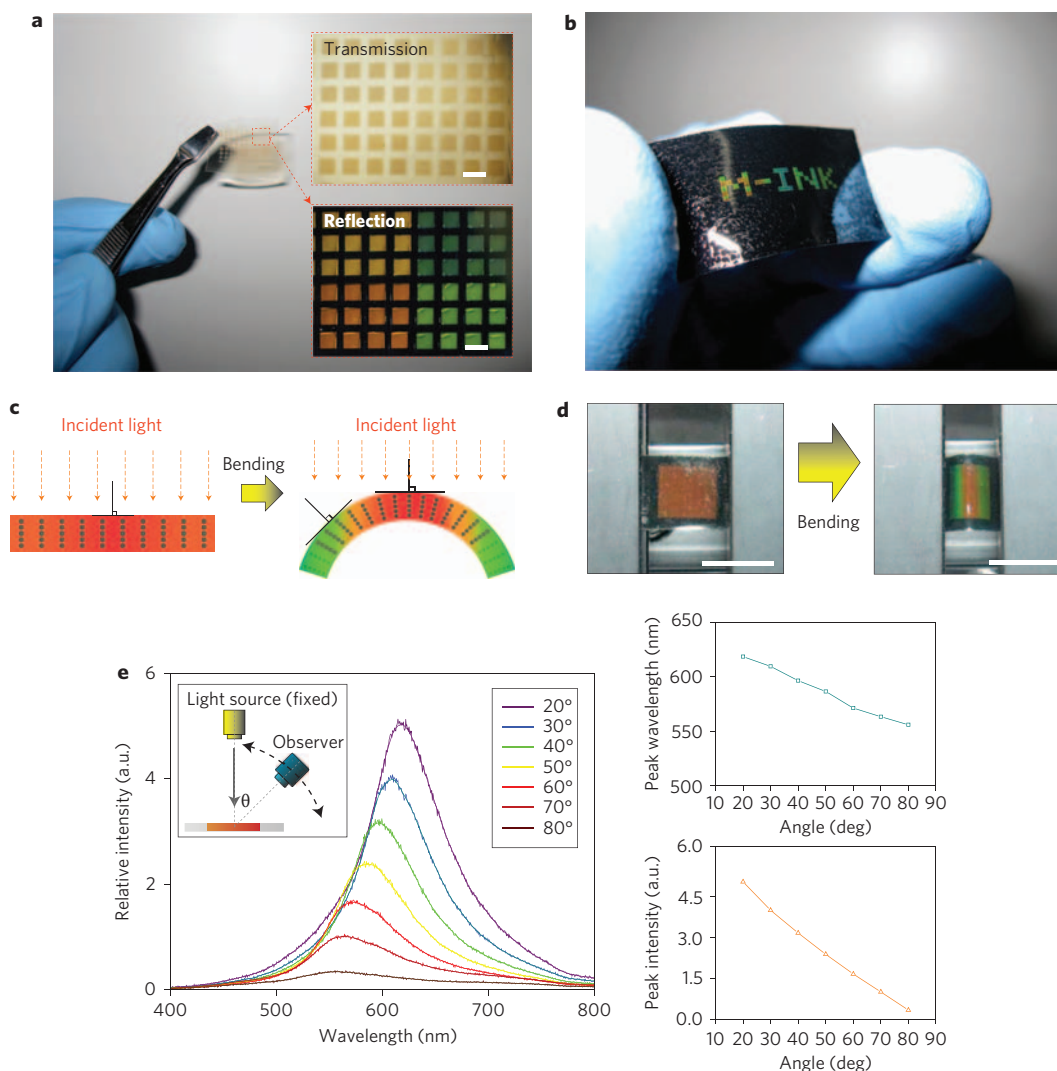


Figure 4 | Flexible photonic crystal thin film and optical properties of the structural colour. **a**, Semi-transparent photonic crystal film (scale bars 400 μm). **b**, Photonic crystal film with anti-transmission black tape as the transferred substrate, which blocks transmission light from the backside. **c**, Schematic of flexible photonic crystal film bending and spectral shift. Variation of curvature results in a change in the angular relationship between the chain-like nanostructure, incident light and the position of the observer. **d**, Mechanical bending of thin-film photonic crystal and related spectral variation with respect to the shorter wavelength. Spectral blueshift occurs when curvature of the film increases owing to the decrease in the optical path length (scale bars 1 cm). **e**, Measurement of viewing angle and plots of peak wavelength and peak intensity versus viewing angle.

structural colours with different geometries and colours (Fig. 2e). For example, the bar-coded microstructures shown in Fig. 2e(iii), composed of 16 colourful strips, were fabricated by 16 sequential colour tuning and fixing steps. Note that there is no alignment error because there is no movement of the substrate during exposure. The width of the bar code is only 10 μm , which demonstrates the high-resolution spatial patterning of the structural colours. Spatial positioning of the smallest feature of structural colour depends on the size of the diffracting unit and the resolution of the lithography processes. Because the size of the CNCs (~ 170 nm) is smaller than the resolution of our optical system, the spatial positioning of the structural colour is mainly determined by the resolution of the optical system, which can be enhanced up to the limit of typical optical lithographic resolutions³⁵.

For a detailed depiction of an image, it is necessary not only to produce structural colour of single colour depth as shown in Fig. 2, but also greyscale modulation and colour mixing, to broaden the facility for colour expression. The proposed scheme for generating structural colour can easily be combined with well-developed reprographic techniques such as half-toning and

dithering^{36,37}, thereby broadening the capability of colour expression. Current digital reprographic techniques express greyscale by varying the density of dots in a pixel that is smaller than the resolution of a human eye. In our case, analogous to traditional greyscale expression, the overall reflection intensity can be modulated by the number of colour dots, and present similar greyscale effects (Fig. 3a). For the proof-of-concept demonstration, we generated 16-pixel arrays, each of them consisting of $25 \mu\text{m} \times 25 \mu\text{m}$ dots for which the configuration was based on the Bayer pattern³⁶ (Fig. 3b). The reflection intensity shown in Fig. 3c verifies 16 distinct intensity levels of corresponding pixel arrays. As an example for reflection intensity modulation, we reproduced a 4-bit monotone image of Mona Lisa, a sixteenth-century Italian portrait by Leonardo da Vinci (Fig. 3d). The reflection intensity of each pixel was modulated by varying the density of dots among 16 levels.

Other than reflection intensity modulation, spatial colour mixing can be achieved by the parallel distribution of colour dots. Quantized dot arrays composed of different colours can be seen as a single mixed colour when their size is below the resolution of the human eye (Fig. 3e). To demonstrate spatial colour mixing of

the structural colour, we fabricated 16-pixel arrays (Fig. 3f). Each pixel was composed of 16 dots of two or three different colours. The spectrum of the colour mixed pixel (Fig. 3g) shows that simple summation of the two different colour spectra results in the total reflection spectrum, proving the spatial mixing of the distinct structural colours. It is interesting to note that this simple spatial mixing scheme of structural colour actually exists in nature. An Indonesian butterfly, *Papilio palinurus*, presents with green on its wings, which results from the spatial mixing of structurally coloured blue and yellow². Following the scheme of spatial colour mixing, as shown in Fig. 3h, we artificially reproduced the butterfly *P. palinurus* by biomimetically mixing structural colours from M-Ink. Magnification of the printed wing area at Fig. 3h shows different colour dots, each of which has dimensions $16.7 \times 16.7 \mu\text{m}^2$ and is well below the resolution of a regular human eye so that spatially distributed dots can be seen as a single mixed colour (Fig. 3i). Spatial colour mixing makes it possible to broaden the expression range of structural colour (see Supplementary Information, Section S4). Because the repetitive tuning and fixing of the photonic nanostructure that we have shown in this work greatly simplifies the manipulation of nanoscale building blocks, in great contrast with the complicated conventional nanofabrication processes, our method enables fast production of structural colours with a high level of controllability.

The nanoparticles embedded in polymeric film can easily be transferred to a flexible substrate (see Supplementary Information, Section S5). Fabricated flexible photonic crystal films are shown in Fig. 4a,b. The colour of the transmission image of the original form of the film is brownish (Fig. 4a). The structural colour of the film is clearly seen by blocking the transmitted light from the back-side by transferring the film to a black substrate (Fig. 4b).

Unlike pigments or dyes, the colour of the patterned M-Ink originates from the chain-like physical structure, thereby demonstrating angular dependency of the colour. The spectra variation occurs in dependence on the angular relationship between the chain-like nanostructure, incident light, and the position of the observer. For example, when the curvature of a flexible photonic crystal film increases, the angle between the vertical plane with respect to the axis of chain and light decreases, so a spectral blueshift occurs (Fig. 4c). We observed the spectral shift with dynamically varying curvature by making use of the mechanical flexibility of the film (Fig. 4d; see also Supplementary Movie S2 and Section S7). The optical characteristics of spectra variation in relation to viewing angle can be seen in Fig. 4e. A detailed discussion of spectral shift along with the various angular relationships may be seen in the Supplementary Information, Section S6. Owing to its unique optical property, our structural colour film can be used as a forgery protection film on currency and various structurally coloured design materials.

In summary, we have demonstrated the first high-resolution patterning of multiple structural colours with a single material, in which the colour is magnetically tunable and lithographically fixable. The versatile material, M-Ink, is developed by magnetically assembling superparamagnetic CNCs into chain-like ordered structures in photocurable resin through the balanced interaction of a magnetically induced attractive force and repulsive forces. A unique immobilization process for the colour of M-Ink, 'tuning and fixing', is developed by taking advantage of the instantaneous nature of the photochemical fixing process. By combining M-Ink and a maskless lithography technique, we have demonstrated the rapid production of high-resolution multicoloured patterns using just a single material and flexible photonic crystals to achieve artificial structural colour. The described approach represents a novel multicolour patterning technique with superior manufacturability, because we can produce colourful patterns conveniently from a single ink instead of using many different inks for different

colours. We believe there is a realizable opportunity to achieve structural colour printing with a fine resolution using this technique. Also, M-Ink-based systems open the door to the widespread use of structural colour for various potential applications including forgery protection, structurally coloured design materials and printing technology.

Methods

Materials. M-Ink is a three-phase mixture of CNCs, solvation liquid and photocurable resin. Superparamagnetic CNCs were synthesized based on a high-temperature hydrolysis reaction followed by a modified Stöber process²⁶, and were initially dispersed in ethanol. CNCs were collected by magnetic separation and re-dispersed in photocurable resin without complete desiccation of the ethanol. Remnant ethanol was used as a solvation liquid (see Supplementary Information, Section S1). We used poly(ethylene glycol) diacrylate (PEG-DA, Sigma-Aldrich, $M_n = 258$) with 15 wt% of photoinitiator (2,2-dimethoxy-2-phenylacetophenone, Sigma-Aldrich) as the photocurable resin. Mixtures of CNCs and photocurable resin were vortexed for 5 min.

Immobilization setup. A NdFeB permanent magnet was used to generate a magnetic field, and was attached to the vertical stage of the microscope. A maskless lithography system was used to cure the resin. The exposure pattern of the UV light was controlled using a digital micromirror array (DMD, Texas Instrument) with a self-designed computer program to synchronize the magnetic actuation, the pattern of the DMD and UV exposure (see Supplementary Information, Section S1).

Optical characterization. Optical micrographs were acquired by a true-colour charge coupled device camera (DP71, Olympus), which was directly aligned to the inverted microscope (IX71, Olympus). Spectrum data were acquired using a spectrometer (Acton, Princeton Instrument), which was connected to the inverted microscope (Eclipse Ti, Nikon). A built-in field stop shutter in the spectrometer was used to isolate the optical signal from background noise and other neighbouring features. Figures 3d,h and 4a,b,d were obtained with a digital camera (IXUS 870 IS, Canon).

Received 19 February 2009; accepted 23 July 2009;
published online 23 August 2009

References

- Srinivasarao, M. Nano-optics in the biological world: beetles, butterflies, birds and moths. *Chem. Rev.* **99**, 1935–1961 (1999).
- Vukusic, P., Sambles, J. R. & Lawrence, C. R. Colour mixing in wing scales of a butterfly. *Nature* **404**, 457 (2000).
- Parker, A. R., McPhedran, R. C., McKenzie, D. R., Botten, L. C. & Nicorovici, N. P. Aphrodite's iridescence. *Nature* **409**, 36–37 (2001).
- Kinoshita, S., Yoshioka, S. & Kawagoe, K. Mechanisms of structural colour in the Morpho butterfly: cooperation of regularity and irregularity in an iridescent scale. *Proc. R. Soc. B* **269**, 1417–1421 (2002).
- Zi, J. *et al.* Coloration strategies in peacock feathers. *Proc. Natl Acad. Sci. USA* **100**, 12576–12578 (2003).
- Potyrailo, R. A. *et al.* Morpho butterfly wing scales demonstrate highly selective vapour response. *Nature Photon.* **1**, 123–128 (2007).
- Braun, P. V. *et al.* Epitaxial growth of high dielectric contrast three-dimensional photonic crystals. *Adv. Mater.* **13**, 721–724 (2001).
- Lee, S., Yi, G. & Yang, S. High-speed fabrication of patterned colloidal photonic structures in centrifugal microfluidic chips. *Lab. Chip* **6**, 1171–1177 (2006).
- Lu, Y., Yin, Y., Gates, B. & Xia, Y. Growth of large crystals of monodispersed spherical colloids in fluidic cells fabricated using non-photolithographic methods. *Langmuir* **17**, 6344–6350 (2001).
- Holgado, M. *et al.* Electrophoretic deposition to control artificial opal growth. *Langmuir* **15**, 4701–4704 (1999).
- Jiang, P., Bertone, J. F., Hwang, K. S. & Colvin, V. L. Single-crystal colloidal multilayers of controlled thickness. *Chem. Mater.* **11**, 2132–2140 (1999).
- Velev, O. D., Lenhoff, A. M. & Kaler, E. W. A class of microstructured particles through colloidal crystallization. *Science* **287**, 2240–2243 (2000).
- Vlasov, Y. A., Bo, X., Sturm, J. C. & Norris, D. J. On-chip natural assembly of silicon photonic bandgap crystals. *Nature* **414**, 289–293 (2001).
- Gu, Z., Fujishima, A. & Sato, O. Fabrication of high-quality opal films with controllable thickness. *Chem. Mater.* **14**, 760–765 (2002).
- Fudouzi, H. & Xia, Y. Colloidal crystals with tunable colors and their use as photonic papers. *Langmuir* **19**, 9653–9660 (2003).
- Prevo, B. G. & Velev, O. D. Controlled, rapid deposition of structured coatings from micro- and nanoparticle suspensions. *Langmuir* **20**, 2099–2107 (2004).
- Masuda, Y., Itoh, T., Itoh, M. & Koumoto, K. Self-assembly patterning of colloidal crystals constructed from opal structure or NaCl structure. *Langmuir* **20**, 5588–5592 (2004).
- Wang, J. *et al.* Simple fabrication of full color colloidal crystal films with tough mechanical strength. *Macromol. Chem. Phys.* **207**, 596–604 (2006).

19. Arsenault, A. C. *et al.* From colour fingerprinting to the control of photoluminescence in elastic photonic crystals. *Nature Mater.* **5**, 179–184 (2006).
20. Arsenault A. C. *et al.* Photonic-crystal full-colour displays. *Nature Photon.* **1**, 468–472 (2007).
21. Huang, J., Wang, X. & Wang, Z. L. Controlled replication of butterfly wings for achieving tunable photonic properties. *Nano Lett.* **6**, 2325–2331 (2006).
22. Saito, A., Yoshioka, S. & Kinoshita, S. Reproduction of the Morpho butterfly's blue: arbitration of contradicting factors. *Proc. SPIE* **5526**, 188–194 (2004).
23. Wong, T., Gupta, M. C., Robins, B. & Levendusky, T. L. Color generation in butterfly wings and fabrication of such structures. *Opt. Lett.* **28**, 2342–2344 (2003).
24. Watanabe, K. *et al.* Optical measurement and fabrication from a Morpho-butterfly-scale quasistructure by focused ion beam chemical vapor deposition. *J. Vac. Sci. Technol. B* **23**, 570–574 (2005).
25. Ge, J., Hu, Y. & Yin, Y. Highly tunable superparamagnetic colloidal photonic crystals. *Angew Chem. Int. Ed.* **46**, 7428–7431 (2007).
26. Ge, J. & Yin, Y. Magnetically tunable colloidal photonic structures in alkanol solutions. *Adv. Mater.* **20**, 3485–3491 (2008).
27. Furst, E. M. & Gast, A. P. Dynamics and lateral interactions of dipolar chains. *Phys. Rev. E* **62**, 6916–6925 (2000).
28. Martin, J. E., Hill, K. M. & Tigges, C. P. Magnetic-field-induced optical transmittance in colloidal suspensions. *Phys. Rev. E* **59**, 5676–5692 (1999).
29. Raghavan, S. R., Walls, H. J. & Khan, S. A. Rheology of silica dispersions in organic liquids: new evidence for solvation forces dictated by hydrogen bonding. *Langmuir* **16**, 7920–7930 (2000).
30. Kobayashi, M., Juillerat, F., Galletto, P., Bowen, P. & Borkovec, M. Aggregation and charging of colloidal silica particles: effect of particle size. *Langmuir* **21**, 5761–5769 (2005).
31. Dickstein, A. J., Erramilli, S., Goldstein, R. E., Jackson, D. P. & Langer, S. A. Labyrinthine pattern formation in magnetic fluids. *Science* **261**, 1012–1015 (1993).
32. Panda, P. *et al.* Stop-flow lithography to generate cell-laden microgel particles. *Lab. Chip* **8**, 1056–1061 (2008).
33. Chung, S. E. *et al.* Optofluidic maskless lithography system for real-time synthesis of photopolymerized microstructures in microfluidic channels. *Appl. Phys. Lett.* **91**, 041106 (2007).
34. Chung, S. E., Park, W., Shin, S., Lee, S. A. & Kwon, S. Guided and fluidic self-assembly of microstructures using railed microfluidic channels. *Nature Mater.* **7**, 581–587 (2008).
35. Ito, T. & Okazaki, S. Pushing the limits of lithography. *Nature* **406**, 1027–1031 (2000).
36. Bayer, B. E. An optimum method for two-level rendition of continuous-tone pictures. *Proc. IEEE Int. Conf. Commun.* **1**, 26–11–26–15 (1973).
37. Ulichney, R. *Digital Halftoning* (MIT Press, 1987).

Acknowledgements

This work was partly supported by the System IC 2010 project of the Ministry of Knowledge Economy and the Nano Systems Institute National Core Research Center (NSI-NCRC) programme of KOSEF. We thank S.E. Chung and N.R. Kim of the School of Electrical Engineering and Computer Science, SNU, for experimental advice. Y.Y. thanks the University of California, Riverside for provision of startup support, and also the Donors of the Petroleum Research Fund, administered by the American Chemical Society, for support of this research.

Author contributions

H.K., Y.Y. and S.K. designed the experiment. H.K., J.G., J.K., S.-e.C., Hosuk L., Howon L. and W.P. performed the experiments and analysis.

Additional information

Supplementary information accompanies this paper at www.nature.com/naturephotonics. Reprints and permission information is available online at <http://npg.nature.com/reprintsandpermissions/>. Correspondence and requests for materials should be addressed to S.K.